university of groningen

University Medical Center Groningen

University of Groningen

The Itaconate Pathway Is a Central Regulatory Node Linking Innate Immune Tolerance and Trained Immunity

Domínguez-Andrés, Jorge; Novakovic, Boris; Li, Yang; Scicluna, Brendon P; Gresnigt, Mark S; Arts, Rob J W; Oosting, Marije; Moorlag, Simone J C F M; Groh, Laszlo A; Zwaag, Jelle

Published in:
Cell metabolism

DOI:
10.1016/j.cmet.2018.09.003

IMPORTANT NOTE: You are advised to consult the publisher's version (publisher's PDF) if you wish to cite from it. Please check the document version below.

Document Version
Publisher's PDF, also known as Version of record

Publication date:
2019

Link to publication in University of Groningen/UMCG research database

Citation for published version (APA):
Domínguez-Andrés, J., Novakovic, B., Li, Y., Scicluna, B. P., Gresnigt, M. S., Arts, R. J. W., Oosting, M., Moorlag, S. J. C. F. M., Groh, L. A., Zwaag, J., Koch, R. M., Ter Horst, R., Joosten, L. A. B., Wijmenga, C., Michelucci, A., van der Poll, T., Kox, M., Pickkers, P., Kumar, V., ... Netea, M. G. (2019). The Itaconate Pathway Is a Central Regulatory Node Linking Innate Immune Tolerance and Trained Immunity. *Cell metabolism*, *29*(1), 211-220.e5. https://doi.org/10.1016/j.cmet.2018.09.003

Copyright
Other than for strictly personal use, it is not permitted to download or to forward/distribute the text or part of it without the consent of the author(s) and/or copyright holder(s), unless the work is under an open content license (like Creative Commons).

The publication may also be distributed here under the terms of Article 25fa of the Dutch Copyright Act, indicated by the “Taverne” license. More information can be found on the University of Groningen website: https://www.rug.nl/library/open-access/self-archiving-pure/taverne-amendment.

Take-down policy
If you believe that this document breaches copyright please contact us providing details, and we will remove access to the work immediately and investigate your claim.

Downloaded from the University of Groningen/UMCG research database (Pure): http://www.rug.nl/research/portal. For technical reasons the number of authors shown on this cover page is limited to 10 maximum.

Short Article

Cell Metabolism

The Itaconate Pathway Is a Central Regulatory Node Linking Innate Immune Tolerance and Trained Immunity

Graphical Abstract

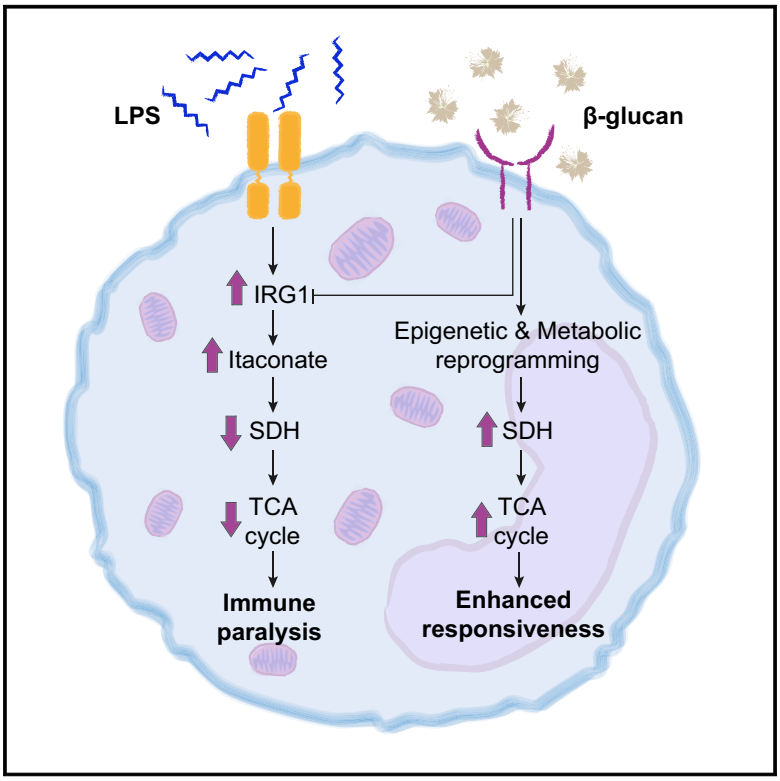

Authors

Jorge Domínguez-Andrés, Boris Novakovic, Yang Li, ..., Vinod Kumar, Henk Stunnenberg, Mihai G. Netea

Correspondence

jorge.dominguezandres@radboudumc.nl

In Brief

Domínguez-Andrés et al. demonstrate the importance of the IRG1-itaconate-SDH axis in the development of immune tolerance and training and highlight the potential of β-glucan-induced trained immunity to revert immunoparalysis, which can occur concurrently with immune hyperactivation in sepsis.

Highlights

- Itaconate is a central component of the inhibitory effects during immune tolerance
- β-Glucan counteracts the tolerizing effects of LPS by inhibiting IRG1 expression
- β-Glucan restores the expression of SDH in tolerant monocytes
- β-Glucan-induced trained immunity has the potential to revert immunoparalysis

Domínguez-Andrés et al., 2019, Cell Metabolism *29*, 211–220
January 8, 2019 © 2018 Elsevier Inc.
https://doi.org/10.1016/j.cmet.2018.09.003

CellPress

Cell Metabolism
Short Article

The Itaconate Pathway Is a Central Regulatory Node Linking Innate Immune Tolerance and Trained Immunity

Jorge Domínguez-Andrés,[1,11,*] Boris Novakovic,[2] Yang Li,[3] Brendon P. Scicluna,[4] Mark S. Gresnigt,[1,10] Rob J.W. Arts,[1] Marije Oosting,[1] Simone J.C.F.M. Moorlag,[1] Laszlo A. Groh,[1] Jelle Zwaag,[5] Rebecca M. Koch,[5] Rob ter Horst,[1] Leo A.B. Joosten,[1] Cisca Wijmenga,[3] Alessandro Michelucci,[6,7] Tom van der Poll,[4] Matthijs Kox,[5] Peter Pickkers,[5] Vinod Kumar,[1,3] Henk Stunnenberg,[2] and Mihai G. Netea[1,8,9]

[1]Department of Internal Medicine (463) and Radboud Center for Infectious Diseases (RCI), Radboud University Nijmegen Medical Centre, Geert Grooteplein 8, Nijmegen 6500 HB, the Netherlands
[2]Department of Molecular Biology, Faculty of Science, Radboud University, Nijmegen 6525 GA, the Netherlands
[3]Department of Genetics, University Medical Center Groningen, Groningen, the Netherlands
[4]Center of Experimental & Molecular Medicine, Division of Infectious Diseases, Amsterdam Medical Center, University of Amsterdam, Amsterdam, the Netherlands
[5]Department of Intensive Care and Radboud Center for Infectious diseases (RCI), Radboud University Nijmegen Medical Centre, Geert Grooteplein 8, Nijmegen 6500 HB, the Netherlands
[6]NORLUX Neuro-Oncology Laboratory, Department of Oncology, Luxembourg Institute of Health, Luxembourg, Luxembourg
[7]Luxembourg Centre for Systems Biomedicine, University of Luxembourg, Esch-Belval, Luxembourg
[8]Department for Genomics & Immunoregulation, Life and Medical Sciences Institute (LIMES), University of Bonn, Bonn, Germany
[9]Human Genomics Laboratory, Craiova University of Medicine and Pharmacy, Craiova, Romania
[10]Department of Microbial Pathogenicity Mechanisms, Leibniz Institute for Natural Product Research and Infection Biology, Hans Knöll Institute, Jena, Germany
[11]Lead Contact
*Correspondence: jorge.dominguezandres@radboudumc.nl
https://doi.org/10.1016/j.cmet.2018.09.003

SUMMARY

Sepsis involves simultaneous hyperactivation of the immune system and immune paralysis, leading to both organ dysfunction and increased susceptibility to secondary infections. Acute activation of myeloid cells induced itaconate synthesis, which subsequently mediated innate immune tolerance in human monocytes. In contrast, induction of trained immunity by β-glucan counteracted tolerance induced in a model of human endotoxemia by inhibiting the expression of immune-responsive gene 1 (IRG1), the enzyme that controls itaconate synthesis. β-Glucan also increased the expression of succinate dehydrogenase (SDH), contributing to the integrity of the TCA cycle and leading to an enhanced innate immune response after secondary stimulation. The role of itaconate was further validated by *IRG1* and *SDH* polymorphisms that modulate induction of tolerance and trained immunity in human monocytes. These data demonstrate the importance of the IRG1-itaconate-SDH axis in the development of immune tolerance and training and highlight the potential of β-glucan-induced trained immunity to revert immunoparalysis.

INTRODUCTION

Sepsis is a clinical condition occurring during severe infections that is characterized by dysregulation of inflammatory responses leading to hypotension, tissue damage, organ dysfunction, and even death. This condition affects between 20 and 30 million people worldwide every year, and it represents a leading cause of death in both developed and developing countries (Martin, 2012). Sepsis is characterized by an exacerbated inflammatory response to infection and, therefore, early antimicrobial treatment is critical to increase the chances of survival (van der Poll et al., 2017). While the induction of tolerance should act as a counter-regulatory mechanism to decrease the potential harmful colateral damage in tissues in response to inflammation, an overly strong or long-lasting activation can subsequently lead to a *de facto* immune paralysis with deleterious effects due to an increased susceptibility to secondary infections (Medzhitov et al., 2012).

A growing number of studies have shown that profound metabolic changes in immune cells occur after exposure to pathogens. This metabolic rewiring modulates both early cytokine production, as well as the establishment of disease tolerance and, eventually, the induction of immunoparalysis (van der Poll et al., 2017). These discoveries regarding the role of cellular metabolism of immune cells offer a whole new set of biological therapeutic targets. Itaconate, a product of the decarboxylation of the TCA cycle intermediate *cis*-aconitate, has recently attracted the attention of the scientific community due to its broad immunomodulatory properties linked to immunological tolerance (Bambouskova et al., 2018; Cordes et al., 2016; Michelucci et al., 2013; Mills et al., 2018). In this report, we describe that lipopolysaccharide (LPS)-induced itaconate production promotes tolerance in human monocytes. In addition, we describe that β-glucan, a fungal cell wall component that exerts a long-term upregulation of innate immune function effects on monocytes

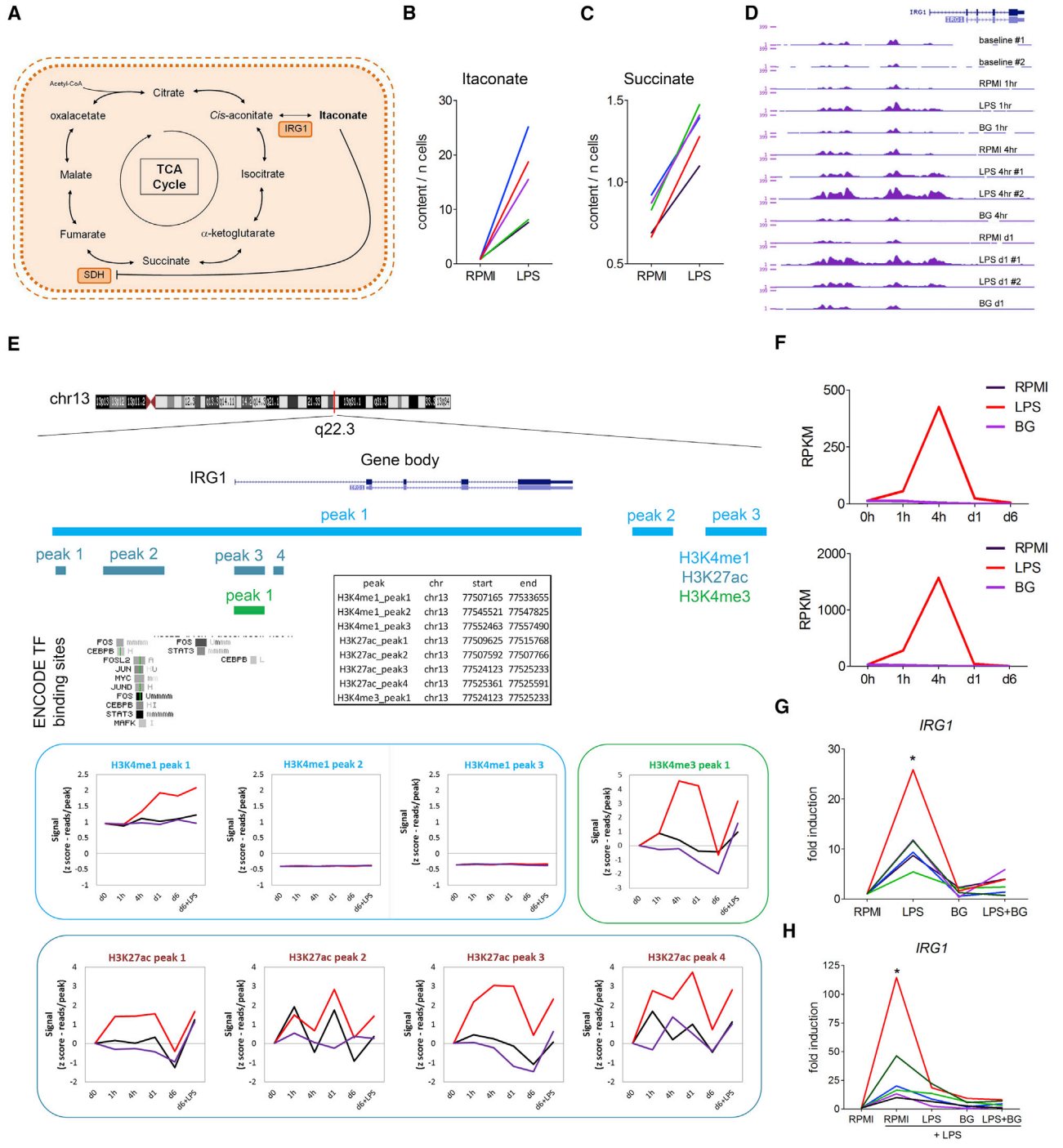

Figure 1. β-Glucan Inhibits *IRG1* Expression after LPS Stimulation

(A) Schematic view of the TCA cycle and the pathways involved in itaconate synthesis.

(B and C) Itaconate (B) and succinate (C) levels in monocytes obtained from blood of volunteers challenged with RPMI or LPS for 2 hr, normalized to cell number (n = 5).

(D) H3K27ac dynamics at *IRG1* locus among monocytes treated with RPMI, LPS, or β-glucan.

(E) Chromatin dynamics of *IRG1* in monocytes after LPS stimulation, shown as mean-centered reads/peak chromatin immunoprecipitation sequencing signal. Coordinates for each peak are shown in hg19 genome build.

(F) Time course RNA expression of *IRG1* in LPS- or β-glucan-treated cells is shown separately for two donors (d0, baseline; 1h, 1 hr; 4h, 4 hr; d1, 24 hr; d6, day 6).

(G) Fold increase of mRNA expression for *IRG1* analyzed by RT-PCR in monocytes 4 hr after stimulation with RPMI, LPS, β-glucan, or LPS + β-glucan is shown separately for six donors. *$p < 0.05$, Wilcoxon signed-rank test.

(legend continued on next page)

and macrophages termed "*trained immunity*" (Quintin et al., 2012), counteracts this effect by maintaining the integrity of the TCA cycle.

By preserving the functionality of succinate dehydrogenase (SDH) pathway, β-glucan-induced trained immunity reverses immune paralysis. These data identify itaconate metabolism as a crucial regulatory node between tolerance and trained immunity and makes it an attractive therapeutic target in sepsis.

RESULTS

β-Glucan Blocks the Induction of the Itaconate Pathway

Itaconate is one of the most strongly upregulated metabolites in activated macrophages, accumulating in high levels after LPS stimulation (Figure 1A) (Lampropoulou et al., 2016). In line with this, we observed an extensive intracellular accumulation of itaconate in monocytes stimulated *ex vivo* with LPS, while the presence of this metabolite in unstimulated cells was barely undetectable (Figure 1B). Intracellular levels of succinate also increased in response to LPS stimulation, as described previously (Figure 1C) (Tannahill et al., 2013). The production of itaconate is dependent on immune-responsive gene 1 (*IRG1*), the gene responsible for encoding the synthesis of the homonymous enzyme, which is necessary for the decarboxylation of *cis*-aconitate to form itaconate (Michelucci et al., 2013).

The analysis of histone 3 lysine 27 acetylation (H3K27ac) patterns of *IRG1* after acute stimulation with microbial ligands revealed that LPS, but not β-glucan, induced a strong H3K27 acetylation around *IRG1* after 1 and 4 hr, and 1 day after LPS stimulation (Figure 1D), which is in line with the expression pattern of *IRG1* and itaconate described previously (Michelucci et al., 2013). The analysis of chromatin dynamics at the *IRG1* locus in monocytes after stimulation led to the observation that the presence of H3K4me3, a mark normally found on active promoters, and H3K27ac, which is generally associated with both enhancers and promoters (Calo and Wysocka, 2013), follow a pattern highly correlated with the active expression of *IRG1* (Figure 1E). In the same line, increase in H3K4me1 at a distal enhancer of *IRG1* is closely related to the timing of the challenges performed.

Strikingly, while LPS dramatically increased the expression of *IRG1* in the first hours after exposure, it did not upregulate the expression of *IRG1* at later time points (day 6) (Figure 1F). Interestingly, stimulation of monocytes from different healthy donors with a combination of LPS and β-glucan only mildly increased *IRG1* levels (Figure 1G), which suggests that β-glucan impaired the LPS-induced expression of *IRG1* in monocytes. In addition, secondary restimulation with LPS of monocytes previously exposed to β-glucan led only to a minor increase in the expression levels of *IRG1*, suggesting a long-lasting effect of β-glucan as an inhibitor of *IRG1* expression (Figure 1H). It has been recently shown that an interferon β feedback loop regulates the itaconate pathway (Mills et al., 2018). The time course expression of *IFNB1* followed an expression pattern similar to IRG1 (Figure S1A). The blockade of the interferon α/β receptor prior to exposure to LPS partly inhibited the development of tolerance in human monocytes (Figures S1B and S1C). Since Nrf2 has been described as a target for itaconate, we analyzed the expression of Nrf2-dependent genes after LPS or β-glucan stimulation. The expression of these genes peaked in the first hours after β-glucan stimulation, tending to become similar to the other conditions after several days of culture (Figure S1D).

Itaconate Inhibits the Induction of Trained Immunity

In accordance with previous reports, we observed that pre-treatment of monocytes with 0.25 μM dimethylitaconate (DMI), a membrane-permeable non-ionic form of itaconate (Lampropoulou et al., 2016), inhibited cytokine production after LPS stimulation without affecting cell viability (Figures S2A–S2C). This immunomodulatory role of DMI led us to test its effects in an established model of trained immunity (Bekkering et al., 2016). β-Glucan induced a significant increase in lactate production after 6 days of culture, which corresponds to a switch to glycolytic metabolism (Cheng et al., 2014), whereas the levels of lactate produced by LPS-tolerized cells remained stable. Addition of β-glucan together with LPS partially reverted the tolerance of monocytes, keeping the cells in a responsive state after 7 days of culture. Conversely, the treatment of monocytes with DMI before training with β-glucan prevented the β-glucan-induced increase in lactate release (Figure 2A) and cytokine production (Figure 2B), illustrating the inhibitory effects of itaconate on trained immunity in human monocytes. Of note, the addition of β-glucan did not revert the tolerance induced by the TLR2 ligand Pam3Cys (Figures S2D and S2E). The utilization of 4-octyl itaconate (OI), a recently described cell-permeable derivative of itaconate with a thiol reactivity similar to itaconate (Mills et al., 2018), led to similar results (Figure S2F).

These results suggest that itaconate exerts an immunomodulatory role through mechanisms that affect cell metabolism. Since it has been previously reported that itaconate is an inhibitor of SDH (Cordes et al., 2016; Lampropoulou et al., 2016), we measured the intracellular levels of succinate and fumarate, the substrate and product involved in the reactions catalyzed by SDH (Rutter et al., 2010). As shown before (Tannahill et al., 2013), treatment of cells with LPS led to the accumulation of succinate 12 hr after stimulation, an effect that was reversed by DMI (Figure 2C). β-Glucan exposure of cells for 24 hr increased succinate and fumarate levels 6 days later, while the combination of LPS and β-glucan only marginally enhanced the production of these TCA cycle metabolites compared with LPS alone. Addition of DMI reversed the accumulation of both succinate and fumarate induced by β-glucan on day 6 after the initial training. OI also induced the accumulation of succinate, albeit to a lower extent (Figure S2G). In line with this, the knockdown of *Irg1* expression in RAW 264.7 cells impaired the accumulation of succinate after acute stimulation of cells with LPS (Figure 2D). The addition of OI to trained monocytes, together with β-glucan, reversed basal oxygen consumption rate and

(H) Fold increase of mRNA expression for *IRG1* analyzed by RT-PCR in monocytes 4 hr after LPS stimulation of cells previously challenged with RPMI, LPS, β-glucan, or LPS + β-glucan 3 days before, is shown separately for six donors.

*$p < 0.05$, Wilcoxon signed-rank test. *IFNB1* expression, effects of interferon α/β receptor blockade and time course expression of Nrf2-dependent genes is displayed in Figure S1.

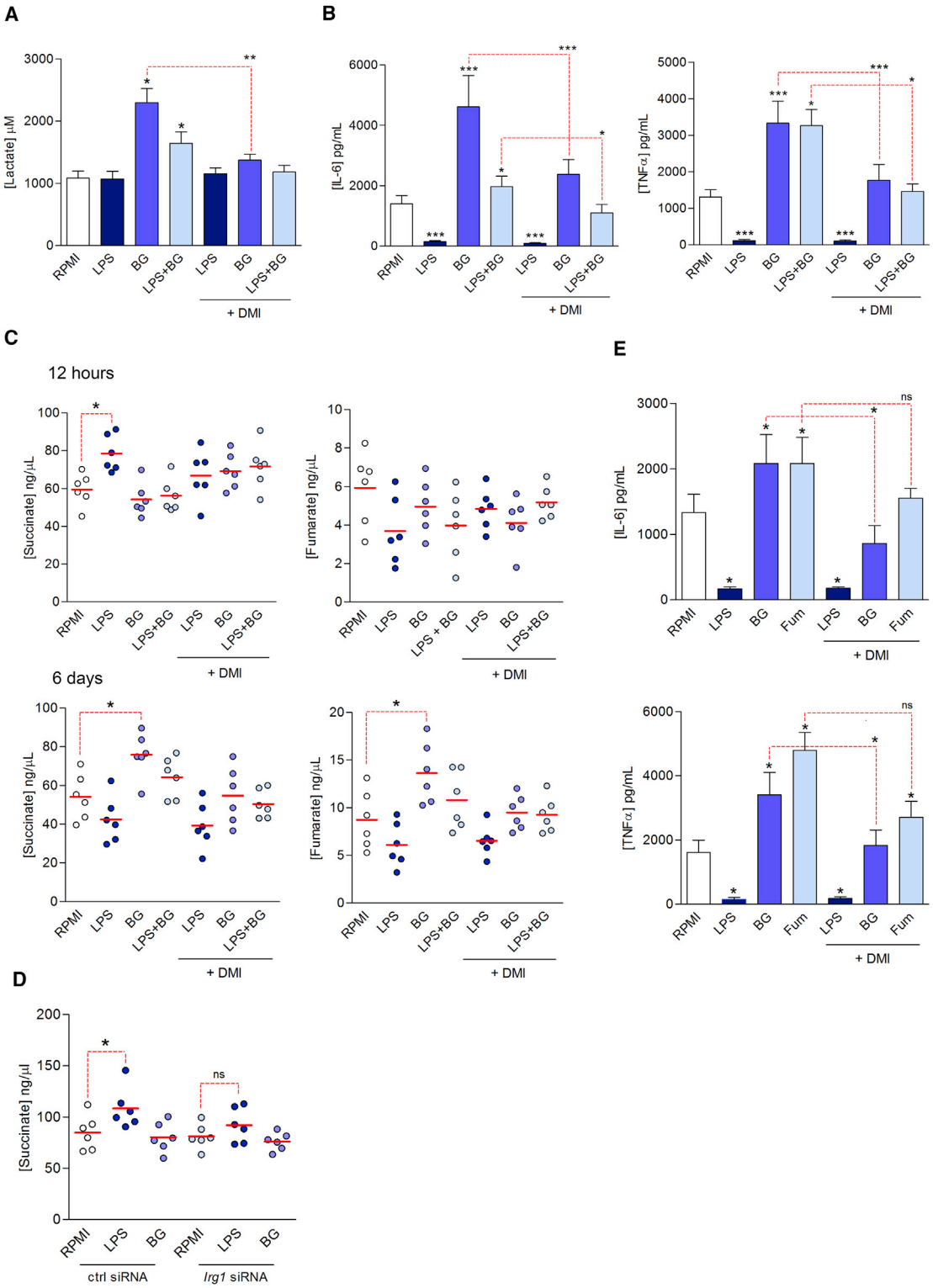

Figure 2. β-Glucan Reverts Itaconate-Induced Tolerance in LPS-Stimulated Monocytes

(A) Lactate production by human monocytes 6 days after 24 hr stimulation with RPMI and LPS, β-glucan, or LPS + β-glucan with or without 0.25 μM dimethylitaconate (DMI), followed by culture media (mean ± SEM, n = 6–12; pooled from two to four independent experiments). *p < 0.05, **p < 0.01 Wilcoxon signed-rank test.

(legend continued on next page)

spare respiratory capacity toward the levels found in homeostasis (Figures S3A–S3D). Reactive oxygen species (ROS) production was not strongly influenced by OI treatment (Figure S3E).

Accumulation of fumarate, which is inhibited by itaconate, has been shown to be a crucial component for the induction of trained immunity (Arts et al., 2016). The addition of methylfumarate, a membrane-permeable form of fumarate, to bypass the inhibition induced by itaconate, was able to revert the decrease in cytokine production induced by DMI in human monocytes (Figure 2E). These results suggest that a functional SDH is crucial for trained immunity, and needed to avoid the induction of tolerance in monocytes after LPS stimulation. The addition of fumarate bypassed the loss of function of SDH in the TCA cycle and thus reverted the tolerance induced by itaconate.

β-Glucan Treatment Restores SDH Expression in Tolerant Monocytes in a Model of *In Vivo* Human Endotoxemia

SDH, also known as mitochondrial complex II, requires the assembly of four different subunits: SDHA, SDHB, SDHC, and SDHD (Bezawork-Geleta et al., 2017). We monitored the time course expression of the four subunits of SDH after LPS or β-glucan challenge: LPS impaired the increase of SDH isoforms normally occurring during monocyte differentiation *in vitro*, while addition of β-glucan to LPS-stimulated monocytes 24 hr after the first challenge enhanced the expression of the four SDH subunits by day 6 (Figure 3A). Figure 3B shows an example of H3K27ac accumulation at the *SDHC* gene during differentiation of monocytes, an effect that is diminished by LPS, suggesting that changes in gene transcription are mediated through epigenetic mechanisms, and future studies are warranted to fully investigate these mechanisms.

We complemented these *in vitro* data with the analysis of the expression of SDH in monocytes obtained from 11 healthy donors who were intravenously challenged by LPS *in vivo*. Monocytes were isolated from blood 4 hr after LPS administration, when they are in a tolerized state (Kox et al., 2011), after which they were exposed to either RPMI or β-glucan *ex vivo* for 24 hr to reverse tolerance. On day 3 they were restimulated with LPS for 4 hr in order to assess their responsiveness (Figure 3C). The exposure of naive monocytes to β-glucan increased SDH expression at a higher extent than RPMI alone (Figure S4A). We observed that an *in vivo* LPS challenge resulted in decreased expression of the four SDH subunits (Figure 3D), whereas β-glucan stimulation reversed this inhibition in the majority of the samples (Figure 3E). To validate the potential of β-glucan to counteract the immunoparalysis in patients, we measured the expression of the different subunits of SDH in monocytes from three intensive care unit sepsis patients before and after *ex vivo* stimulation with LPS or β-glucan. In these patients, β-glucan increased the expression of SDH subunits (Figure 3F). These results underline the importance of the IRG1-itaconate-SDH axis in the development of tolerance after LPS challenge and highlight the potential of β-glucan as a tool to revert immunoparalysis.

SNPs in *IRG1*, *SDHA*, *SDHB*, *SDHC*, and *SDHD* Influence Induction of Trained Immunity and Tolerance in Human Volunteers

To validate the role of itaconate as a regulator of trained immunity and tolerance, we analyzed the link between inflammatory gene expression and the presence of expression quantitative trait loci (eQTLs) (Albert and Kruglyak, 2015) for these genes using blood RNA sequencing data from 627 individuals from the LLdeep cohort of Western Europeans (Tigchelaar et al., 2015). All the genes of interest had at least one suggestive *cis*-eQTL (Figure 4A). The boxplot of the most significant eQTL per gene is also shown in the analysis (Figure 4B). This strategy allowed us to select a series of SNPs that affected the expression of *IRG1*, *SDHA*, *SDHB*, *SDHC*, and *SDHD*. The effect of these SNPs in trained immunity or tolerance was subsequently validated in monocytes from the 200FG cohort of the Human Functional Genomics Project (Li et al., 2016), according to the protocol described by Bekkering et al. (2016). Cytokine and lactate production was assessed after exposure of monocytes to either β-glucan or Bacillus Calmette-Guérin (both inducing trained immunity), or LPS or *Borrelia burgdorferi* (inducing tolerance), followed by restimulation at day 6 with LPS. Several SNPs in all the genes of interest had an impact on the production of lactate, interleukin-6, and tumor necrosis factor alpha after restimulation with LPS, concluding that these regions of the genome are quantitative trait loci for the induction of trained immunity and tolerance (Figures 4C and S3). In addition to this, the intersection of the trained immunity QTLs with the *cis*-eQTLs led to the identification of several SNPs in *SDHA* that influenced both cytokines and gene expression (Figure S4B). Collectively, these results underline the central role played by the itaconate pathway genes *IRG1* and *SDH* for the induction of trained immunity and tolerance.

DISCUSSION

Innate immune tolerance induced during severe infections is a powerful mechanism that can provide protection against colateral damage caused by exacerbated inflammatory responses within the first hours of sepsis (Medzhitov et al., 2012). The

(B) Interleukin-6 (IL-6) and tumor necrosis factor alpha (TNF-α) production by human monocytes treated or not with 0.25 μM DMI and stimulated with RPMI, LPS, β-glucan, or LPS + β-glucan for 24 hr, followed by culture media. After 6 days, monocytes were re-exposed to LPS, and cytokines were measured 24 hr later (mean ± SEM, n = 6–12; pooled from two to four independent experiments). *p < 0.05, ***p < 0.001, Wilcoxon signed-rank test.

(C) Intracellular succinate and fumarate levels of monocytes 12 hr and 6 days after RPMI and LPS, β-glucan, or LPS + β-glucan with or without 0.25 μM DMI followed by culture media (mean, n = 6; pooled from two independent experiments). *p < 0.05, Wilcoxon signed-rank test.

(D) Intracellular succinate levels of *Irg1* small interfering RNA (siRNA)- or control siRNA-transfected RAW 264.7 cells 12 hr after RPMI, LPS, or β-glucan stimulation (mean, n = 6) *p < 0.05, Wilcoxon signed-rank test.

(E) IL-6 and TNF-α production by human monocytes treated or not with 0.25 μM DMI and stimulated with RPMI, LPS, β-glucan, or 50 μM methylfumarate (Fum) for 24 hr followed by culture media. After 6 days, monocytes were re-exposed to LPS, and cytokines were measured 24 hr later (mean, n = 6; pooled from two to four independent experiments). *p < 0.05, Wilcoxon signed-rank test.

Results of 24 hr stimulation, titration of DMI, cytotoxicity assays, stimulation with Pam3Cys, and experiments with OI are displayed in Figure S2.

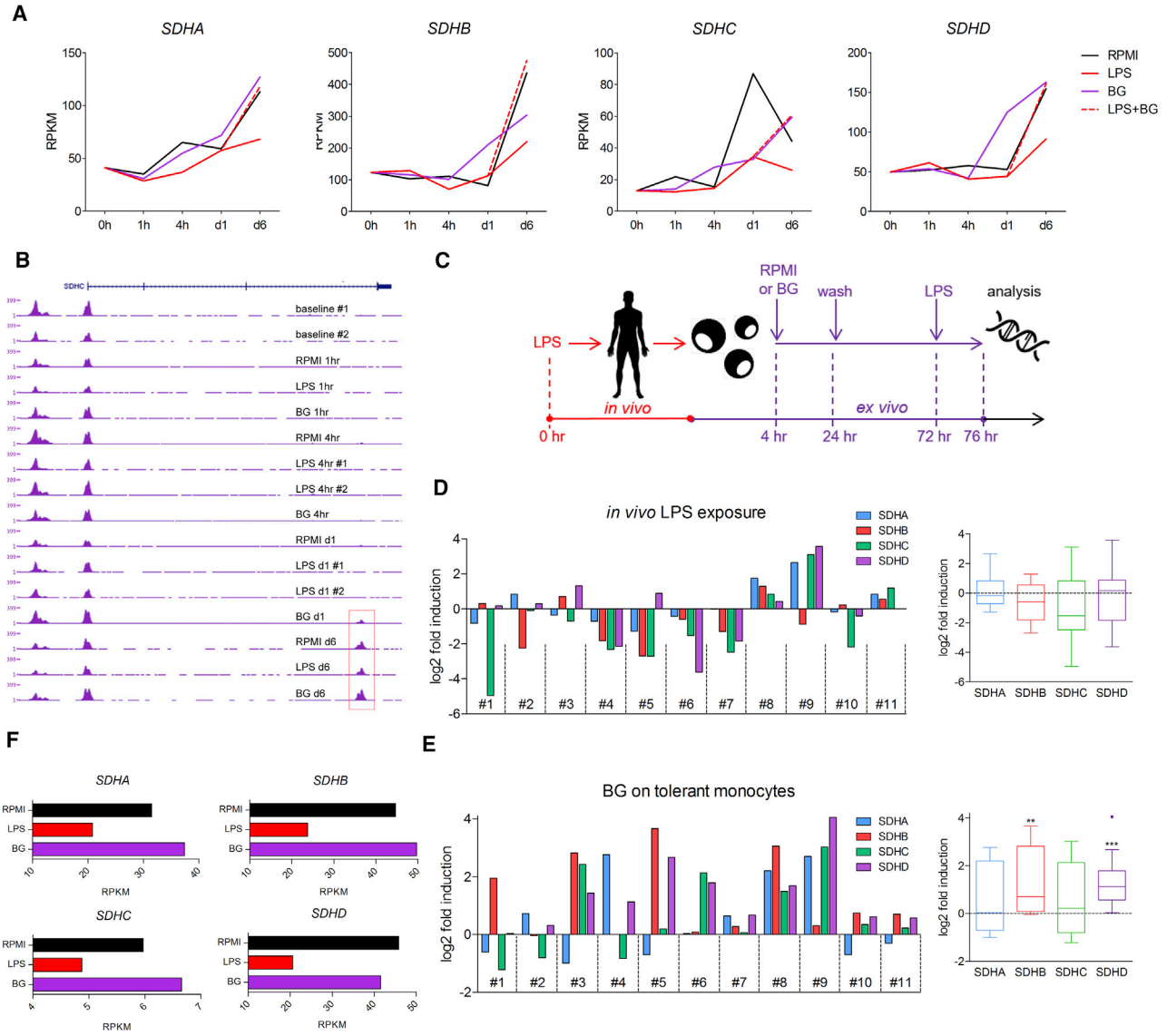

Figure 3. β-Glucan Increases H3K27Ac of *SDH* Locus and mRNA Expression in Tolerized Human Monocytes

(A) Time course expression of *SDHA*, *SDHB*, *SDHC*, and *SDHD* in cells stimulated with RPMI, LPS, or β-glucan (BG) for 24 hr, followed by culture media. In LPS + BG-treated cells, BG was added 24 hr after exposure to LPS (mean values, n = 5).

(B) H3K27ac dynamics at *SDHC* in monocytes treated with RPMI, LPS, or BG.

(C) Scheme of the procedure followed in (D and E).

(D and E) Effect of *in vivo* LPS exposure on the expression of *SDHA*, *SDHB*, *SDHC*, and *SDHD* in monocytes from 11 healthy donors. Log2 fold change expression naive *in vivo* (D), or log2 fold change expression BG-RPMI exposed after 3 days in culture (E) (data displayed in boxes as mean ± SEM, n = 11. **p < 0.01, ***p < 0.001 Wilcoxon signed-rank test).

(F) Expression of *SDHA*, *SDHB*, *SDHC*, and *SDHD* in monocytes isolated from three sepsis patients and exposed to RPMI, LPS, or BG for 4 hr (mean values, n = 3). See also Figure S4A.

induction of *IRG1*, leading to the formation of itaconate, has been suggested to be an important component of this response (Mills et al., 2018; Nair et al., 2018). However, inappropriate activation of these processes can lead to a functional state of immunoparalysis that can be deleterious to the host as a result of increased susceptibility toward secondary infections (Cheng et al., 2016; van der Poll et al., 2017). Recently, induction of trained immunity by β-glucan was shown to reverse immune paralysis in monocytes in a human experimental model of sepsis, a process accompanied by profound metabolic rewiring of circulating monocytes (Novakovic et al., 2016). In this study, we demonstrate that the itaconate synthesis pathway represents an important regulatory node for induction of tolerance and regulation of trained immunity.

The innate immune system reacts to the infection in a rapid but uncontrolled way, generating a powerful inflammatory response

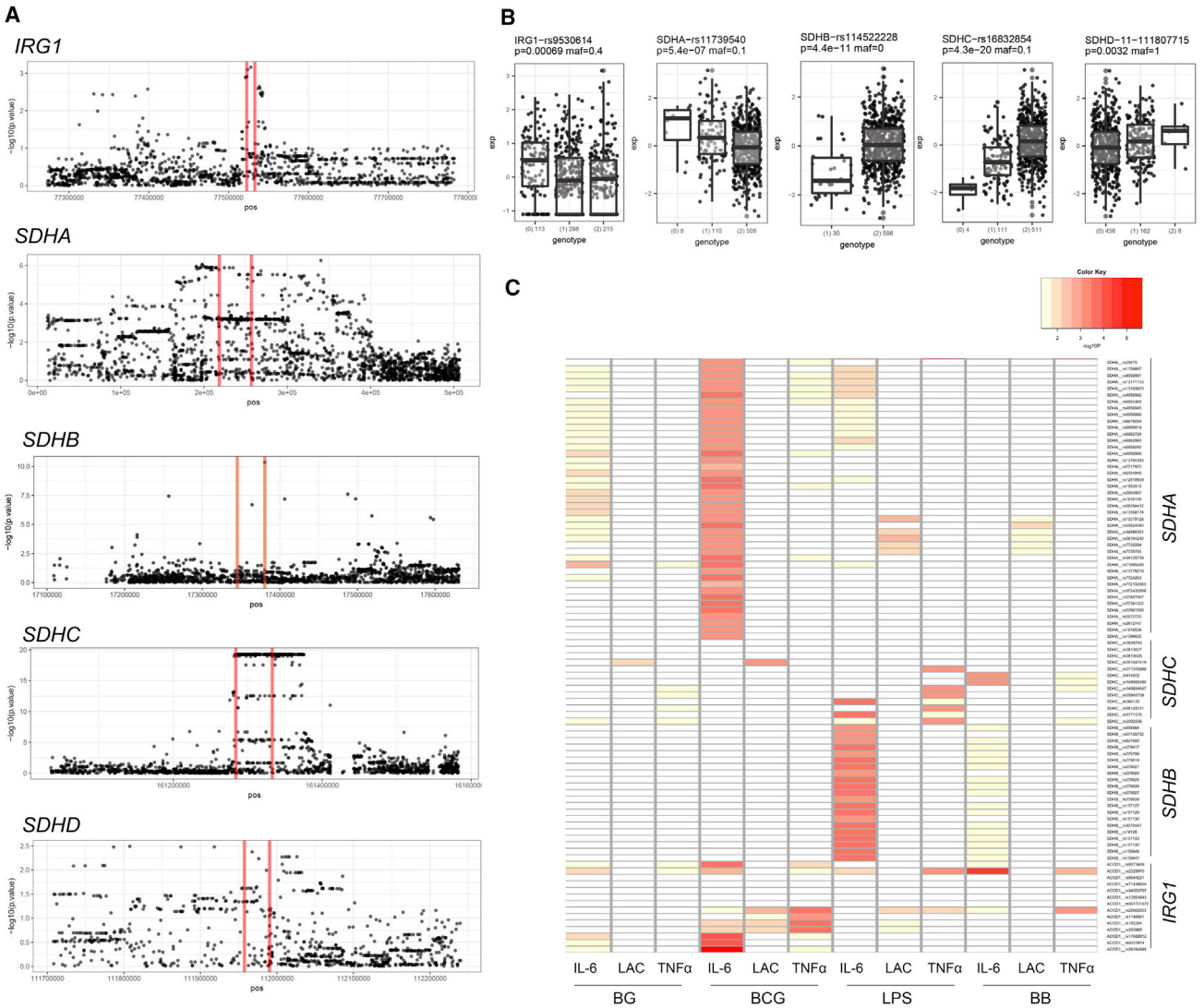

Figure 4. SNPs at *IRG1*, *SDHA*, *SDHB*, *SDHC*, and *SDHD* Loci Are QTLs for the Induction of Trained Immunity or Tolerance

(A) *cis*-eQTL results for *IRG1*, *SDHA*, *SDHB*, *SDHC*, and *SDHD* using blood RNA sequencing data from 627 LLdeep samples. In the plots, red vertical lines show start and end of the gene. The y axis shows the –log10p value of eQTL for all SNPs around the gene.

(B) Boxplot of the most significant eQTL per gene.

(C) Changes in IL-6, TNF-α, or lactate production related with previously described SNPs in the genes of interest after BG + LPS, Bacillus Calmette-Guérin (BCG) + LPS, LPS + LPS, or *Borrelia burgdorferi* (BB) + LPS stimulation in monocytes from the 200FG cohort of the Human Functional Genomics Project. See also Figure S4B.

(Dominguez-Andres and Netea, 2018). This process also induces robust histone acetylation around *IRG1* in the first 24 hr, resulting in a strong upregulation of its expression and triggering the synthesis of high amounts of itaconate. In turn, itaconate induces tolerance by inhibiting cytokine production, thus contributing to the reversal toward homeostasis (Li et al., 2013). LPS stimulation dampens the activity of the TCA cycle and induces the accumulation of succinate (Tannahill et al., 2013) by a mechanism dependent on the SDH-inhibitory action of itaconate (Cordes et al., 2016; Lampropoulou et al., 2016). In this study we show that treatment of monocytes with β-glucan inhibits the LPS-induced expression of *IRG1*, blocking the potentially deleterious effects of itaconate on immunoparalysis, which is in line with the reported protective actions of β-glucan in animal models of sepsis (Bedirli et al., 2007; Şener et al., 2005). In addition, inhibitory effects on *IRG1* may also explain the capacity of β-glucan to reverse the epigenetic state of LPS-induced tolerance (Novakovic et al., 2016). Recent research has identified Nrf2 as a target for itaconate (Mills et al., 2018). However, we observed that, in the context of trained immunity and tolerance, no major changes in target genes of Nrf2 take place, suggesting that the effects mediated by the itaconate the context of long-term tolerance are mostly Nrf2 independent. This possibility is supported by a recent study reporting both Nrf2-dependent and Nrf2-indpendent biological effects of itaconate (Bambouskova et al., 2018).

At the epigenetic level, the persistence of H3K4me1 marks around *IRG1* after the first stimulation is in agreement with the reported presence of H3K4me1 at enhancers, even after their disengagement and loss of activation potential (Bogdanovic et al., 2012). In line with this, the pre-existing H3K4 methylation allows the acquisition of H3K27ac, a mark associated with active enhancers, as the latter is acquired almost exclusively in the presence of the former (Calo and Wysocka, 2013).

The tolerizing effects of itaconate are long-lasting, impairing not only the acute LPS-induced cytokine production, but also the enhancement of glycolytic metabolism and cytokine production capacity observed during the development of β-glucan-induced trained immunity (Netea et al., 2016). Interestingly, the concentrations of succinate and fumarate in cells treated with itaconate underwent fewer changes than those treated with LPS, arguing that itaconate mainly influences the induction of inflammation during stimulation, rather than the steady-state metabolism of the cell. Since the effects of itaconate on cellular metabolism are thought to be mediated through SDH inhibition, hampering the transformation of succinate into fumarate (Cordes et al., 2016; Lampropoulou et al., 2016), we assessed whether fumarate can bypass the inhibitory effects induced by itaconate. Indeed, fumarate bypassed the SDH blockade and reverted the tolerizing effects of itaconate treatment, in agreement with a previous report showing that fumarate itself is able to induce trained immunity in human monocytes (Arts et al., 2016). Our data add further weight to the concept that SDH is a regulatory hub linking metabolism and inflammation: through its regulatory role on TCA cycle and oxidative phosphorylation (Mills and O'Neill, 2014), regulating the levels of succinate and ROS (Domínguez-Andrés et al., 2017), SDH exerts a strong influence on inflammatory cell behavior (Mills et al., 2016). In our study we report that LPS blocks SDH activity through induction of itaconate. On the other hand, β-glucan-induced trained immunity increases the H3K27ac at the level of *SDH* and amplifies the expression of the different SDH subunits, restoring the metabolic plasticity of the cells (Lussey-Lepoutre et al., 2015), the pro-inflammatory cytokine production (Mills et al., 2016), and subsequently re-establishing the immunocompetence of cells.

An additional validation arguing for the importance of the IRG1-itaconate-SDH axis for the modulation of cytokine production is given by the demonstration that both trained immunity and tolerance induction are strongly influenced by genetic polymorphisms in loci situated in *IRG1*, *SDHA*, *SDHB*, *SDHC*, and *SDHD*. Numerous SNPs in these genes directly correlate with significant quantitative changes in the production of pro-inflammatory cytokines during induction of trained immunity and tolerance. The specificity of various QTLs in the SDH subunits for either trained immunity or tolerance remains to be explained, and is likely to be the source of interesting biology that warrants further investigation in future studies not only in the field of innate immune memory, but also in other contexts such as adaptive immunity or self-tolerance. Indeed, one can envisage modulatory effects of itaconate on the adaptive immune responses mediated by lymphocytes as well.

In conclusion, itaconate induction is a crucial component of the inhibitory effects on cytokine production during innate immune tolerance, and β-glucan can counteract this effect by inhibitory effects on IRG1 expression. By preserving the functionality of the SDH pathway through epigenetic mechanisms, β-glucan-induced trained immunity can reverse immune paralysis. These data identify itaconate metabolism as a crucial regulatory node between tolerance and trained immunity, and makes it an attractive therapeutic target in sepsis, and possibly other conditions associated with altered innate immune responses, such as cancer, in which immunosuppression bears many similarities with sepsis-derived immunoparalysis (Rosolem et al., 2012). Also, itaconate could be employed as a potential therapeutic tool in conditions where the induction of trained immunity can result in negative consequences, such as autoimmune diseases and inflammatory disorders.

Limitations of Study

A comprehensive understanding of the intracellular and extracellular activities of itaconate and its derivatives is indispensable for the design of therapeutic interventions based on this pathway. One of the limitations of our study is that it has been carried out in blood monocytes, which is a convenient model, but it does not offer a broad assessment of the potential effects of itaconate in different tissues and organs. In addition, we employed compounds with a structure similar to that of itaconate, such as OI and DMI, which have allowed us to mimic the effects of the endogenous itaconate. However, these compounds could also present additional pharmacological effects due to their different chemical structure and electrophilicity. Additional future work should address these limitations in order to provide an improved understanding of how the itaconate pathway modulates innate immune memory and tolerance in different clinically relevant scenarios.

STAR★METHODS

Detailed methods are provided in the online version of this paper and include the following:

- KEY RESOURCES TABLE
- CONTACT FOR REAGENT AND RESOURCE SHARING
- METHOD DETAILS
  - Monocyte Isolation
  - Monocyte Trained Immunity and Tolerance Experiments
  - Healthy Volunteers Endotoxemia Experiments
  - Itaconate and Succinate Measurements
  - Cytokine Measurements
  - Metabolite Measurements
  - mRNA Extraction and RT-PCR
  - Viability Assays
  - Chromatin Immunoprecipitation
  - RNA Sequencing Data from In Vitro Cultured Monocytes
  - RNA Sequencing Data from Experimental Human Endotoxemia Model
  - Sepsis Patient Data
  - RNA-seq Library Preparation and Sequencing
  - Genetic Analysis 200FG Cohort
  - eQTL Analysis
  - Metabolic Analysis
  - RNA Interference

- IFNAR Blockade
- ROS Production
- Statistical Analysis
- Accession Numbers

SUPPLEMENTAL INFORMATION

Supplemental Information includes four figures and can be found with this article online at https://doi.org/10.1016/j.cmet.2018.09.003.

ACKNOWLEDGMENTS

We thank Richard C. Hartley for 4-octyl itaconate. This study was partly supported by TOP grants from the Netherlands Organization for Scientific Research (to M.G.N., H.S., and T.v.d.P.). M.G.N. was supported by an ERC Consolidator Grant (no. 310372) and by a Spinoza Grant from the Netherlands Organisation for Scientific Research. B.N. is supported by an NHMRC (Australia) CJ Martin Fellowship.

AUTHOR CONTRIBUTIONS

Conceptualization, J.D.-A., B.N., L.A.B.J., and M.G.N.; Methodology, J.D.-A., B.N., Y.L., B.P.S., M.S.G., R.J.W.A., M.O., S.J.C.F.M.M., L.A.G., R.t.H., M.K., V.K., and A.M.; Investigation, J.D.-A., B.N., Y.L., B.P.S., M.S.G., R.J.W.A., M.O., S.J.C.F.M.M., L.A.G., J.Z., R.M.K., M.K., and V.K.; Writing – Original Draft: J.D.-A., B.N., and M.G.N.; Writing – Review & Editing, J.D.-A., B.N., Y.L., M.S.G., R.J.W.A., M.O., S.J.C.F.M.M., M.K., V.K., H.S., and M.G.N.; Supervision, L.A.B.J., C.W., T.v.d.P., M.K., P.P., V.K., H.S., and M.G.N.

DECLARATION OF INTERESTS

The authors declare no competing interests.

Received: March 20, 2018
Revised: July 18, 2018
Accepted: September 3, 2018
Published: October 4, 2018

REFERENCES

Albert, F.W., and Kruglyak, L. (2015). The role of regulatory variation in complex traits and disease. Nat. Rev. Genet. *16*, 197–212.

Arts, R.J.W., Novakovic, B., ter Horst, R., Carvalho, A., Bekkering, S., Lachmandas, E., Rodrigues, F., Silvestre, R., Cheng, S.-C., Wang, S.-Y., et al. (2016). Glutaminolysis and fumarate accumulation integrate immunometabolic and epigenetic programs in trained immunity. Cell Metab. *24*, 807–819.

Bambouskova, M., Gorvel, L., Lampropoulou, V., Sergushichev, A., Loginicheva, E., Johnson, K., Korenfeld, D., Mathyer, M.E., Kim, H., Huang, L.-H., et al. (2018). Electrophilic properties of itaconate and derivatives regulate the IκBζ–ATF3 inflammatory axis. Nature *556*, 501–504.

Barnett, D.W., Garrison, E.K., Quinlan, A.R., Stromberg, M.P., and Marth, G.T. (2011). BamTools: a C++ API and toolkit for analyzing and managing BAM files. Bioinformatics *27*, 1691–1692.

Bedirli, A., Kerem, M., Pasaoglu, H., Akyurek, N., Tezcaner, T., Elbeg, S., Memis, L., and Sakrak, O. (2007). Beta-glucan attenuates inflammatory cytokine release and prevents acute lung injury in an experimental model of sepsis. Shock *27*, 397–401.

Bekkering, S., Blok, B.A., Joosten, L.A.B., Riksen, N.P., van Crevel, R., and Netea, M.G. (2016). In vitro experimental model of trained innate immunity in human primary monocytes. Clin. Vaccine Immunol. *23*, 926–933.

Bezawork-Geleta, A., Rohlena, J., Dong, L., Pacak, K., and Neuzil, J. (2017). Mitochondrial complex II: at the crossroads. Trends Biochem. Sci. *42*, 312–325.

Bogdanovic, O., Fernandez-Minan, A., Tena, J.J., de la Calle-Mustienes, E., Hidalgo, C., van Kruysbergen, I., van Heeringen, S.J., Veenstra, G.J.C., and Gomez-Skarmeta, J.L. (2012). Dynamics of enhancer chromatin signatures mark the transition from pluripotency to cell specification during embryogenesis. Genome Res. *22*, 2043–2053.

Calo, E., and Wysocka, J. (2013). Modification of enhancer chromatin: what, how, and why? Mol. Cell *49*, 825–837.

Cheng, S.-C., Quintin, J., Cramer, R.A., Shepardson, K.M., Saeed, S., Kumar, V., Giamarellos-Bourboulis, E.J., Martens, J.H.A., Rao, N.A., Aghajanirefah, A., et al. (2014). mTOR- and HIF-1α-mediated aerobic glycolysis as metabolic basis for trained immunity. Science *345*, 1250684.

Cheng, S.-C., Scicluna, B.P., Arts, R.J.W., Gresnigt, M.S., Lachmandas, E., Giamarellos-Bourboulis, E.J., Kox, M., Manjeri, G.R., Wagenaars, J.A.L., Cremer, O.L., et al. (2016). Broad defects in the energy metabolism of leukocytes underlie immunoparalysis in sepsis. Nat. Immunol. *17*, 406–413.

Cordes, T., Wallace, M., Michelucci, A., Divakaruni, A.S., Sapcariu, S.C., Sousa, C., Koseki, H., Cabrales, P., Murphy, A.N., Hiller, K., et al. (2016). Immunoresponsive gene 1 and itaconate inhibit succinate dehydrogenase to modulate intracellular succinate levels. J. Biol. Chem. *291*, 14274–14284.

Dominguez-Andres, J., and Netea, M.G. (2018). Long-term reprogramming of the innate immune system. J. Leukoc. Biol. https://doi.org/10.1002/JLB.MR0318-104R.

Domínguez-Andrés, J., Arts, R.J.W., ter Horst, R., Gresnigt, M.S., Smeekens, S.P., Ratter, J.M., Lachmandas, E., Boutens, L., van de Veerdonk, F.L., Joosten, L.A.B., et al. (2017). Rewiring monocyte glucose metabolism via C-type lectin signaling protects against disseminated candidiasis. PLoS Pathog. *13*, e1006632.

Heinz, S., Benner, C., Spann, N., Bertolino, E., Lin, Y.C., Laslo, P., Cheng, J.X., Murre, C., Singh, H., and Glass, C.K. (2010). Simple combinations of lineage-determining transcription factors prime cis-regulatory elements required for macrophage and B cell identities. Mol. Cell *38*, 576–589.

Kox, M., de Kleijn, S., Pompe, J.C., Ramakers, B.P., Netea, M.G., van der Hoeven, J.G., Hoedemaekers, C.W., and Pickkers, P. (2011). Differential ex vivo and in vivo endotoxin tolerance kinetics following human endotoxemia. Crit. Care Med. *39*, 1866–1870.

Kox, M., van Eijk, L.T., Zwaag, J., van den Wildenberg, J., Sweep, F.C.G.J., van der Hoeven, J.G., and Pickkers, P. (2014). Voluntary activation of the sympathetic nervous system and attenuation of the innate immune response in humans. Proc. Natl. Acad. Sci. USA *111*, 7379–7384.

Lachmandas, E., Beigier-Bompadre, M., Cheng, S.-C., Kumar, V., van Laarhoven, A., Wang, X., Ammerdorffer, A., Boutens, L., de Jong, D., Kanneganti, T.-D., et al. (2016). Rewiring cellular metabolism via the AKT/mTOR pathway contributes to host defence against Mycobacterium tuberculosis in human and murine cells. Eur. J. Immunol. *46*, 2574–2586.

Lampropoulou, V., Sergushichev, A., Bambouskova, M., Nair, S., Vincent, E.E.E., Loginicheva, E., Cervantes-Barragan, L., Ma, X., Huang, S.C.-C.C.-C., Griss, T., et al. (2016). Itaconate links inhibition of succinate dehydrogenase with macrophage metabolic remodeling and regulation of inflammation. Cell Metab. *24*, 158–166.

Langmead, B., Trapnell, C., Pop, M., and Salzberg, S.L. (2009). Ultrafast and memory-efficient alignment of short DNA sequences to the human genome. Genome Biol. *10*, R25.

Li, Y., Zhang, P., Wang, C., Han, C., Meng, J., Liu, X., Xu, S., Li, N., Wang, Q., Shi, X., et al. (2013). Immune responsive gene 1 (IRG1) promotes endotoxin tolerance by increasing A20 expression in macrophages through reactive oxygen species. J. Biol. Chem. *288*, 16225–16234.

Li, Y., Oosting, M., Deelen, P., Ricaño-Ponce, I., Smeekens, S., Jaeger, M., Matzaraki, V., Swertz, M.A., Xavier, R.J., Franke, L., et al. (2016). Inter-individual variability and genetic influences on cytokine responses to bacteria and fungi. Nat. Med. *22*, 952–960.

Li, H., and Durbin, R. (2009). Fast and accurate short read alignment with Burrows-Wheeler transform. Bioinformatics *25*, 1754–1760.

Lussey-Lepoutre, C., Hollinshead, K.E.R., Ludwig, C., Menara, M., Morin, A., Castro-Vega, L.-J., Parker, S.J., Janin, M., Martinelli, C., Ottolenghi, C., et al. (2015). Loss of succinate dehydrogenase activity results in dependency on pyruvate carboxylation for cellular anabolism. Nat. Commun. *6*, 8784.

Martin, G.S. (2012). Sepsis, severe sepsis and septic shock: changes in incidence, pathogens and outcomes. Expert Rev. Anti Infect. Ther. *10*, 701–706.

Medzhitov, R., Schneider, D.S., and Soares, M.P. (2012). Disease tolerance as a defense strategy. Science *335*, 936–941.

Michelucci, A., Cordes, T., Ghelfi, J., Pailot, A., Reiling, N., Goldmann, O., Binz, T., Wegner, A., Tallam, A., Rausell, A., et al. (2013). Immune-responsive gene 1 protein links metabolism to immunity by catalyzing itaconic acid production. Proc. Natl. Acad. Sci. USA *110*, 7820–7825.

Mills, E., and O'Neill, L.A.J. (2014). Succinate: a metabolic signal in inflammation. Trends Cell Biol. *24*, 313–320.

Mills, E.L.L., Kelly, B., Logan, A., Costa, A.S.H.S.H., Varma, M., Bryant, C.E.E., Tourlomousis, P., Däbritz, J.H.M.H.M., Gottlieb, E., Latorre, I., et al. (2016). Succinate dehydrogenase supports metabolic repurposing of mitochondria to drive inflammatory macrophages. Cell *167*, 457–470.e13.

Mills, E.L., Ryan, D.G., Prag, H.A., Dikovskaya, D., Menon, D., Zaslona, Z., Jedrychowski, M.P., Costa, A.S.H., Higgins, M., Hams, E., et al. (2018). Itaconate is an anti-inflammatory metabolite that activates Nrf2 via alkylation of KEAP1. Nature *556*, 113–117.

Nair, S., Huynh, J.P., Lampropoulou, V., Loginicheva, E., Esaulova, E., Gounder, A.P., Boon, A.C.M., Schwarzkopf, E.A., Bradstreet, T.R., Edelson, B.T., et al. (2018). Irg1 expression in myeloid cells prevents immunopathology during M. tuberculosis infection. J. Exp. Med. *215*, 1035–1045.

Netea, M.G., Joosten, L.A.B., Latz, E., Mills, K.H.G., Natoli, G., Stunnenberg, H.G., ONeill, L.A.J., and Xavier, R.J. (2016). Trained immunity: a program of innate immune memory in health and disease. Science *352*, aaf1098.

Novakovic, B., Habibi, E., Wang, S.-Y., Arts, R.J.W., Davar, R., Megchelenbrink, W., Kim, B., Kuznetsova, T., Kox, M., Zwaag, J., et al. (2016). β-Glucan reverses the epigenetic state of LPS-induced immunological tolerance. Cell *167*, 1354–1368.e14.

Quinlan, A.R., and Hall, I.M. (2010). BEDTools: a flexible suite of utilities for comparing genomic features. Bioinformatics *26*, 841–842.

Quintin, J., Saeed, S., Martens, J.H.A., Giamarellos-Bourboulis, E.J., Ifrim, D.C., Logie, C., Jacobs, L., Jansen, T., Kullberg, B.-J., Wijmenga, C., et al. (2012). *Candida albicans* infection affords protection against reinfection via functional reprogramming of monocytes. Cell Host Microbe *12*, 223–232.

Repnik, U., Knezevic, M., and Jeras, M. (2003). Simple and cost-effective isolation of monocytes from buffy coats. J. Immunol. Methods *278*, 283–292.

Ricaño-Ponce, I., Zhernakova, D.V., Deelen, P., Luo, O., Li, X., Isaacs, A., Karjalainen, J., Di Tommaso, J., Borek, Z.A., Zorro, M.M., et al. (2016). Refined mapping of autoimmune disease associated genetic variants with gene expression suggests an important role for non-coding RNAs. J. Autoimmun. *68*, 62–74.

Robinson, M.D., and Oshlack, A. (2010). A scaling normalization method for differential expression analysis of RNA-seq data. Genome Biol. *11*, R25.

Rosolem, M.M., Rabello, L.S.C.F., Lisboa, T., Caruso, P., Costa, R.T., Leal, J.V.R., Salluh, J.I.F., and Soares, M. (2012). Critically ill patients with cancer and sepsis: clinical course and prognostic factors. J. Crit. Care *27*, 301–307.

Rutter, J., Winge, D.R., and Schiffman, J.D. (2010). Succinate dehydrogenase - assembly, regulation and role in human disease. Mitochondrion *10*, 393–401.

Saeed, S., Quintin, J., Kerstens, H.H.D., Rao, N.A., Aghajanirefah, A., Matarese, F., Cheng, S.-C., Ratter, J., Berentsen, K., van der Ent, M.A., et al. (2014). Epigenetic programming of monocyte-to-macrophage differentiation and trained innate immunity. Science *345*, 1251086.

Şener, G., Toklu, H., Ercan, F., and Erkanlı, G. (2005). Protective effect of β-glucan against oxidative organ injury in a rat model of sepsis. Int. Immunopharmacol. *5*, 1387–1396.

Tannahill, G.M., Curtis, A.M., Adamik, J., Palsson-McDermott, E.M., McGettrick, A.F., Goel, G., Frezza, C., Bernard, N.J., Kelly, B., Foley, N.H., et al. (2013). Succinate is an inflammatory signal that induces IL-1β through HIF-1α. Nature *496*, 238–242.

Tigchelaar, E.F., Zhernakova, A., Dekens, J.A.M., Hermes, G., Baranska, A., Mujagic, Z., Swertz, M.A., Muñoz, A.M., Deelen, P., Cénit, M.C., et al. (2015). Cohort profile: LifeLines DEEP, a prospective, general population cohort study in the northern Netherlands: study design and baseline characteristics. BMJ Open *5*, e006772.

van der Poll, T., van de Veerdonk, F.L., Scicluna, B.P., and Netea, M.G. (2017). The immunopathology of sepsis and potential therapeutic targets. Nat. Rev. Immunol. *17*, 407–420.

Ward, L.D., and Kellis, M. (2012). HaploReg: a resource for exploring chromatin states, conservation, and regulatory motif alterations within sets of genetically linked variants. Nucleic Acids Res. *40*, D930–D934.

Wu, T.D., and Nacu, S. (2010). Fast and SNP-tolerant detection of complex variants and splicing in short reads. Bioinformatics *26*, 873–881.

Zhang, Y., Liu, T., Meyer, C.A., Eeckhoute, J., Johnson, D.S., Bernstein, B.E., Nussbaum, C., Myers, R.M., Brown, M., Li, W., et al. (2008). Model-based analysis of ChIP-seq (MACS). Genome Biol. *9*, R137.

Zhu, C.T., and Rand, D.M. (2012). A hydrazine coupled cycling assay validates the decrease in redox ratio under starvation in *Drosophila*. PLoS One *7*, e47584.

STAR★METHODS

KEY RESOURCES TABLE

REAGENT or RESOURCE	SOURCE	IDENTIFIER
Antibodies		
α-IFN-alpha/beta R1 antibody	R&D Systems	AF3039; RRID:AB_664107
IgG isotype control	R&D Systems	AB-108-C; RRID:AB_354267
Rabbit polyclonal anti-H3K27ac	Diagenode	pAb-196-050; RRID:AB_2637079
Rabbit polyclonal anti-H3K4me1	Diagenode	pAb-037-050; RRID:AB_2561054
Rabbit polyclonal anti-H3K4me3	Diagenode	pAb-003-050; RRID:AB_2616052
Chemicals, Peptides, and Recombinant Proteins		
Gentamycin	Thermo Fisher Scientific	15750060
Lipopolysaccharide from *E. coli* serotype 055:B5	Sigma-Aldrich	L2880
Pam3Cys	EMC Microcollections	L2000
Percoll	Sigma-Aldrich	P1644
Ficoll-Paque	GE Healthcare	17-1440-03
Roswell Park Memorial Institute medium (RPMI)	Invitrogen	22406031
$CD14^+$ beads	MACS Miltenyi	130-050-201
TRIzol reagent	Life Technologies	15596018
SYBR Green	Applied Biosciences	4368708
16% Formaldehyde	Fisher Scientific	28908, 11835835
Protein A/G Magnetic beads	Diagenode	C03010021-150
β1,3-(D)glucan (β-glucan)	Saeed et al., 2014	N/A
Mono methyl-fumarate	Sigma-Aldrich	651419-1G
Dimethylitaconate	Sigma-Aldrich	592498-25G
4-octyl itaconate	Mills et al., 2018	
IRG1 siRNA (mouse)	Santa Cruz	sc-146287
control siRNA (mouse)	Santa Cruz	sc-37007
siRNA Transfection Medium	Santa Cruz	sc-36868
siRNA Dilution Buffer	Santa Cruz	sc-29527
siRNA Transfection Reagent	Santa Cruz	sc-29528
Seahorse XF Base Medium	Agilent Technologies	102353-100
Bovine Serum Albumin (BSA)	Sigma-Aldrich	A7030
Luminol	Sigma-Aldrich	A8511-5G
Zymosan (from *S. cerevisiae*)	Sigma-Aldrich	Z4250-1G
Critical Commercial Assays		
Human TNFα ELISA	R&D systems	DY210
Human IL-6 ELISA	R&D systems	DY206
Lactate Fluorometric Assay Kit	Biovision	K607
iScript cDNA Synthesis Kit	Bio-Rad	1708891
Succinate Colometric Assay kit	Sigma-Aldrich	MAK184
Glutamate Assay Kit	Sigma-Aldrich	MAK004
CytoTox 96 Non-Radioactive Cytotoxicity Assay	Promega	G1780
Rneasy Mini Kit	QIAGEN	74106
KAPA library preparation kit	Kapa Biosystems	KK8400
riboZero gold rRNA removal kit	Illumina	MRZG12324
Second Strand Buffer	Life Technologies	10812-014
Superscript III Reverse Transcriptase	Life Technologies	18080-044

(*Continued on next page*)

Continued

REAGENT or RESOURCE	SOURCE	IDENTIFIER
Ribozero Gold Kit	Illumina	MRZG12324
Qubit RNA HS assay kit Ribozero	Life Technologies	Q32852
DNase I	QIAGEN	79254
Sodium Acetate (3M)	Life Technologies	AM9740
iQ SYBR Green Supermix	Bio-Rad	1708880
Nextera DNA Library Prep Kit	Illumina	FC-121-1031
TruSeq SBS KIT v3 - HS (50 cycles)	Illumina	FC-401-3002
NextSeq 500/550 High Output v2 kit (75 cycles)	Illumina	FC-404-2005
NEBNext High-Fidelity 2 3 PCR Master Mix	New England Biolabs	M0541
100 x SYBR Green I Nucleic Acid Gel Stain	Thermo Fisher Scientific	S7563
SPRIselect reagent kit	Beckman Coulter	B23218
E-Gel SizeSelect Agarose Gels, 2%	Thermo Fisher Scientific	G661002
dNTP set 100 mM	Life Technologies	10297-018
dUTP 100 mM	Promega	U119A
Glycogen (20 mg/mL)	Life Technologies	10814-010
Random Hexamer primers	Sigma-Aldrich	11034731001
DNA polymerase I, *E. coli*	New England Biolabs	M0209S
USER enzyme	New England Biolabs	M5505L
E. coli Ligase	New England Biolabs	M0205L
Rnasin Plus Rnase Inhibitor	Promega	N2615
Ribonuclease H	Life Technologies	AM2293
T4 DNA polymerase	New England Biolabs	M0203L
Ribozero Gold Kit	Illumina	MRZG12324
Deposited Data		
Raw data files for ChIP sequencing	Novakovic et al., 2016	GSE85245
Raw data files for RNA sequencing	Novakovic et al., 2016	GSE85243
Raw data files for β-glucan and LPS SuperSeries data	Novakovic et al., 2016	GSE85246
Experimental Models: Cell Lines		
Mouse: RAW264.7 cells	ATCC	TIB-71
Experimental Models: Organisms/Strains		
Human: 200FG cohort (Human Functional Genomics project)	Li et al., 2016	http://www.humanfunctionalgenomics.org
Human: LLDeep cohort	Tigchelaar et al., 2015	
Human: primary monocytes from healthy volunteers	Sanquin Blood Bank	
Oligonucleotides		
Primer *HPRT* fw 5'-CCTGGCGTCGTGATTAGTGAT-3'	Sigma-Aldrich	Designed by BLAST
Primer *HPRT* rv 5'-AGACGTTCAGTCCTGTCCATAA-3'	Sigma-Aldrich	Designed by BLAST
Primer *IRG1* fw 5'-GTTCCTGGGAACCACTACG-3'	Lachmandas et al., 2016	
Primer *IRG1* rv 5'-GATGTCTGGCTGACCCCAAA-3'	Lachmandas et al., 2016	
Primer *IFNB1* fw 5'-ATGACCAACAAGTGTCTCCTCC-3'	Sigma-Aldrich	Designed by BLAST
Primer *IFNB1* rv 5'-GGAATCCAAGCAAGTTGTAGCTC-3'	Sigma-Aldrich	Designed by BLAST
Software and Algorithms		
NanoDrop software	N/A	N/A
GraphPad Prism	Graphpad Software	https://www.graphpad.com
Bedtools	Quinlan and Hall, 2010	http://bedtools.readthedocs.io/en/latest/; http://research-pub.gene.com/gmap
Bamtools	Barnett et al., 2011	https://github.com/pezmaster31/bamtools
Samtools	Li and Durbin, 2009	http://samtools.sourceforge.net

(*Continued on next page*)

Continued

REAGENT or RESOURCE	SOURCE	IDENTIFIER
GSNAP	Wu and Nacu, 2010	http://research-pub.gene.com/gma
HOMER	Heinz et al., 2010	http://homer.salk.edu/homer/motif
Bowtie	Langmead et al., 2009	http://bowtie-bio.sourceforge.net/index.shtml
MACS2	Zhang et al., 2008	https://github.com/taoliu/MACS

CONTACT FOR REAGENT AND RESOURCE SHARING

Further information and requests for reagents may be directed to the Lead Contact, Jorge Domínguez-Andrés (jorge.dominguezandres@radboudumc.nl).

METHOD DETAILS

Monocyte Isolation

Buffy coats from healthy donors were obtained after written informed consent (Sanquin Blood Bank, Nijmegen, the Netherlands). Samples were anonymized to safeguard donor privacy. The use of the samples received IRB approval. Percoll isolation of monocytes was performed as previously described (Repnik et al., 2003). Briefly, 150 - 200 x 10^6 PBMCs were layered on top of a hyper-osmotic Percoll solution (48.5% Percoll (Sigma-Aldrich), 41.5% sterile H2O, and 0.16 M filter-sterilized NaCl) and centrifuged for 15 min at 580g. The interphase layer was isolated and cells were washed with cold PBS. Cells were re-suspended in RPMI culture medium (RPMI medium Dutch modified, Invitrogen) supplemented with 50 μg/mL gentamicin, 2 mM Glutamax, and 1 mM pyruvate, and counted. An extra purification step was added by adhering Percoll-isolated monocytes to polystyrene flat bottom plates (Corning) for 1 hr at 37°C; a washing step with warm PBS was then performed to yield maximal purity.

Monocyte Trained Immunity and Tolerance Experiments

100 μL monocytes at 1 x 10^6 cells/mL were added to flat-bottom 96-well plates (Greiner). Cells were stimulated with 10 ng/mL *E. coli* LPS (serotype 055:B5, Sigma-Aldrich, 10 ng/mL), 5 μg/mL β-glucan (β-1,3-(D)-glucan, kindly provided by Professor David Williams), 10 ng/mL *E. coli* LPS + 1 μg/mL β-glucan, 50 μM mono-methylfumarate (Sigma), or 10 μg/mL Pam3Cys (EMC Microcollections). Supernatants from monocytes were collected 24 hr after stimulation. Cells were washed once with 200 μL warm PBS and incubated for 5 days in culture medium with 10% serum and medium was changed once. Cells were restimulated with 10 ng/mL *E. coli* LPS. After 24 h, supernatants were collected and stored at -20°C. In some experiments, cells were preincubated (before first stimulation) for 1 hr with 0.25 μM dimethylitaconate (Sigma) or 100 μM 4-octyl itaconate, kindly provided by Professor Richard C. Hartley. Concentration of dimethylitaconate was selected as being the highest non-cytotoxic concentration (see Figure S1 and Lampropoulou et al., 2016). All supernatants were stored at -20°C until analysis.

Healthy Volunteers Endotoxemia Experiments

In vivo LPS-induced endotoxemia was performed at the Radboud University Medical Center, Nijmegen, the Netherlands as part of the randomised, placebo-controlled FLUENZ-trial (registered at ClinicalTrials.gov as NCT02642237). After approval from the local ethics committee (CMO 2015/2058), eleven healthy, non-smoking, Caucasian, male volunteers between the ages of 18 and 35 years were admitted and monitored at the intensive care unit for one day. All volunteers gave written informed consent beforehand and all experiments were conducted in accordance with the Declaration of Helsinki. Subjects were screened through normal physical examination, electrocardiography, and routine laboratory values (including serology on HIV and hepatitis B). Exclusion criteria included febrile illness two weeks before baseline, a suspicion of influenza infection in the preceding year, pre-existent (lung) disease, recent vaccination and usage of any prescription drugs. Subjects refrained from caffeine and alcohol 24 hr before experiments and from food 12 hr before experiments, as well as during experiments. Experimental human endotoxemia was conducted as described previously (Kox et al., 2014). Volunteers were intravenously infused with a bolus *E. coli* LPS (2 ng/kg; US Standard Reference Endotoxin O:113; Pharmaceutical Development Section of the National Institutes of Health (Bethesda, MD)).

Itaconate and Succinate Measurements

$CD14^+$ monocytes were isolated from the PBMC fraction using magnetic beads labeled with anti-$CD14^+$ (MACS Miltenyi, Cologne, Germany) according to the manufacturer's protocol. Unstimulated and stimulated $CD14^+$ monocytes pellets were adjusted to 2x10^6/mL in nitrogen snap frozen and shipped to Metabolon (Morrisville, U.S.) for metabolic profiling.

Cytokine Measurements

Cytokine production from human cells was determined in supernatants using commercial ELISA kits for IL-6 and TNFα (R&D Systems, Minneapolis, MN) following the instructions of the manufacturer.

Metabolite Measurements

Lactate was measured from cell culture supernatants using a coupled enzymatic assay in which lactate was oxidized and the resulting H_2O_2 was coupled to the conversion of Amplex Red reagent to fluorescent resorufin by HRP (horseradish peroxidase) (Zhu and Rand, 2012). Glutamate and succinate concentrations were determined by commercial assay kits (Sigma) following the instructions of the manufacturer from at least one million monocytes lysed in 1 mL 0.5% Triton-X in PBS at 12 hr and 6 days after stimulation.

mRNA Extraction and RT-PCR

Cells were cultured as described above. mRNA was extracted by TRIzol (Life Technologies), according to the manufacturer's instructions, and cDNA was synthesized using iScript reverse transcriptase (Invitrogen). Relative mRNA levels were determined using the Applied Biosciences StepOne PLUS and the SYBR Green method (Invitrogen). Values are expressed as fold increases in mRNA levels, relative to those in non-stimulated cells, with HPRT as housekeeping gene.

Viability Assays

Cell viability was assessed using CytoTox 96 Non-Radioactive Cytotoxicity Assay (Promega). The assay measures lactate dehydrogenase (LDH), a stable cytosolic enzyme that is released upon cell lysis. Released LDH in culture supernatants is measured with a 30-minute coupled enzymatic assay, which results in conversion of a tetrazolium salt (INT) into a red formazan product. The amount of color formed is proportional to the number of lysed cells.

Chromatin Immunoprecipitation

Purified cells were fixed with 1% formaldehyde (Sigma) at a concentration of approximately 10^6 cells/mL. Fixed cell preparations were sonicated using a Diagenode Bioruptor UCD-300 for 3x 10 min (30 s on; 30 s off). 67 mL of chromatin (1 million cells) was incubated with 229 mL dilution buffer, 3 mL protease inhibitor cocktail and 0.5-1 mg of H3K27ac, H3K4me3, H3K4me1, H3K27me3, H3K9me3 or H3K36me3 antibodies (Diagenode) and incubated overnight at 4°C with rotation. Protein A/G magnetic beads were washed in dilution buffer with 0.15% SDS and 0.1% BSA, added to the chromatin/antibody mix and rotated for 60 min at 4°C. Beads were washed with 400ml buffer for 5 min at 4C with five rounds of washes. After washing chromatin was eluted using elution buffer for 20 min. Supernatant was collected, 8 mL 5M NaCl, 3 mL proteinase K were added and samples were incubated for 4 hr at 65°C. Finally, samples were purified using QIAGEN; Qiaquick MinElute PCR purification Kit and eluted in 20 mL EB. Detailed protocols can be found on the Blueprint website (http://www.blueprint-epigenome.eu/UserFiles/file/Protocols/Histone_ChIP_May2013.pdf).

RNA Sequencing Data from In Vitro Cultured Monocytes

For gene expression analysis of *in vitro* monocyte exposure to LPS, BG, and sequential LPS-then-BG, we used previously published RNA-seq data (Novakovic et al., 2016). Briefly, monocytes were differentiated into resting macrophages by *ex vivo* culture in RPMI 1640 medium Dutch modification (Sigma Aldrich) with 10% Human Serum. Media was supplemented with 10 μg/mL gentamycin, 2 mM L-glutamine and 1 mM pyruvate (Life Technologies). Monocytes were exposed to either 10-100ng/mL LPS or 5 μg/mL BG, and collected 4 hr and 24 hr after exposure. Establishment of tolerance or training in the resulting macrophages at day 6 was determined by TNFα and IL-6 release at 24 hr following LPS stimulation using ELISA.

RNA Sequencing Data from Experimental Human Endotoxemia Model

In vivo endotoxin tolerance was examined in 11 healthy nonsmoking volunteers as previously described. Subjects used in this study were previously profiled for cytokine release (Novakovic et al., 2016) and RNA-seq was generated subsequently.

Sepsis Patient Data

Patients with bacterial sepsis admitted to Critical Care at Radboud UMC were used in this study. Blood was collected at day 5 post admission, during the 'tolerant' state. Peripheral blood mononuclear cells were isolated by centrifugation in Ficoll-Paque (GE Healthcare), followed by removal of T cells using an additional Percoll gradient. Monocytes were purified from PBMCs using negative selection in an LD column magnet separator, with beads for $CD3^+$ (T cells), $CD19^+$ (B cells) and $CD56^+$ (NK cells) positive cells (Miltenyi Biotech), yielding >95% pure monocytes.

RNA-seq Library Preparation and Sequencing

Total RNA was extracted from cells using the Qiagen RNeasy RNA extraction kit (Qiagen, Netherlands), using on-column DNAseI treatment. Ribosomal RNA was removed using the riboZero rRNA removal kit (Illumina). RNA was then fragmented into 200bp fragments by incubation for 7.5 min at 95°C in fragmentation buffer (200 mM Tris-acetate, 500 mM Potassium Acetate, 150 mM - Magnesium Acetate, pH 8.2). First strand cDNA synthesis was performed using SuperScript III (Life Technologies), followed by synthesis of the second cDNA strand. Library preparation was performed using the KAPA hyperprep kit (KAPA Biosystems). Quality of cDNA and the efficiency of ribosomal RNA removal was confirmed using quantitative RT-PCR using the IQ Sybr Supermix, with primers for GAPDH, 18S and 28S rRNA. Illumina library preparation was done using the Kapa Hyper Prep Kit, as described previously (Novakovic et al., 2016).

Genetic Analysis 200FG Cohort

The 200FG cohort comprises healthy individuals of Western European descent which gave written informed consent to donate venous blood to use for research (Li et al., 2016). Volunteers were between 23-73 years old, and consisted of 77% males and 23% females. *Ex vivo* trained immunity experiments were performed as described above. SNP information was extracted from a genome-wide Illumina Infinium single-nucleotide polymorphism (SNP) array. Samples with a call rate $\leq$ 0.99 were excluded, as were variants with a Hardy-Weinburg equilibrium (HWE) $\leq$ 0.0001, and minor allele frequency (MAF) $\leq$ 0.001. Raw cytokine levels were first log-transformed then ratios relative to the measurements in culture medium (negative control) was computed. The ratio data were mapped to genotype data using a linear regression model with age and gender as covariates. R-package Matrix-eQTL, was used for QTL mapping, where linear model was applied with age and gender included as co-variables. Experiments were conducted according to the principles expressed in the Declaration of Helsinki.

eQTL Analysis

We used the LLDeep cohort (Tigchelaar et al., 2015), composed of 627 healthy Dutch volunteers, to test for possible eQTL effects of SNPs of interest. For LLDeep, both gene expression data (obtained through RNA-seq) and genotype information are available (Tigchelaar et al., 2015). We mapped eQTLs by a linear model using TMM-normalized (Robinson and Oshlack, 2010) expression data to the genotype information The eQTL mapping strategy and data have been described in detail (Ricaño-Ponce et al., 2016). Briefly, cis-eQTL analysis was performed on transcript-SNP combinations for which the distance from the center of the transcript to the genomic location of the SNP was $\leq$ 500 kb. Associations were tested by non-parametric Spearman's rank correlation test and a p value $<$ 0.05 was considered significant. We also employed HaploReg database v4.1 (Ward and Kellis, 2012) (www.broadinstitute.org/mammals/haploreg/haploreg.php) to extract publicly available eQTL results from blood tissue for cytokine QTL SNPs.

Metabolic Analysis

1×10^7 monocytes were trained in 10 cm Petri dishes (Greiner) in 10 mL of RPMI medium with or without stimuli for 24h, washed with warm PBS and incubated in RPMI culture medium at 37°C, 5% CO2. Following 5 days in culture, cells were detached with Versene solution (ThermoFisher Scientific) and 1×10^5 cells were plated to overnight-calibrated cartridges in assay medium (DMEM with 0.6 mM glutamine, 5 mM glucose and 1 mM pyruvate [pH adjusted to 7.4]) and incubated for 1h in a non-CO2-corrected incubator at 37°C. Oxygen consumption rate (OCR) and extracellular acidification rate (ECAR) were measured using a Cell Mito Stress Kit (for OCR) kit in an XFp Analyzer (Seahorse Bioscience), with final concentrations of 1 μM oligomycin, 1 μM FCCP, and 0.5 μM rotenone/antimycin A.

RNA Interference

Predesigned siRNAs were purchased from Santa Cruz Biotechnology. RAW264.7 cells (5×10^5/mL) were cultured in six-well plates for 6 hr and the transfected with IRG1 siRNA (100 nM) or control siRNA (100 nM) using siRNA Transfection Medium (Santa Cruz) following the instructions of the manufacturer.

IFNAR Blockade

For IFNAR blockade experiments, monocytes were preincubated for 1 hr with 5 μg/mL α-IFN-alpha/beta R1 antibody (R&D systems) and IgG isotype control (R&D systems).

ROS Production

Oxygen radical production levels of isolated monocytes were evaluated using luminol-enhanced chemiluminescence and determined in an automated LB96V Microlumat plus luminometer (EG&GBerthold, Bald Wilberg, Germany). 6-day trained monocytes (1×10^5 per well) were incubated in medium containing either RPMI or opsonized zymosan (1 mg/ml). Luminol was added to each well in order to start the chemiluminescence reaction. Each measurement was carried out in at least duplicate repetitions. Chemiluminescence was determined every 145 s at 37°C for 1 hr. Luminescence was expressed as relative light units (RLU) per second.

Statistical Analysis

Data are presented as mean ± SEM, as indicated in the legend of each fig, unless otherwise stated. The significance of the differences between groups was evaluated using Wilcoxon signed-rank test. Data are judged to be statistically significant when $p < 0.05$ by two-tailed Student's t test. In figures, asterisks denote statistical significance (*, $p < 0.05$; **, $p < 0.01$; ***, $p < 0.001$). For eQTL analysis, associations were tested by non-parametric Spearman's rank correlation test and a p value $<$0.05 was considered significant. Statistical parameters including the exact value of n, precision measures (mean ± SEM) and statistical significance are reported in the figures and the figure legends when necessary. Statistical analysis was performed in GraphPad PRISM 6.

Accession Numbers

The accession numbers for the RNA sequencing time course of control, β-glucan-trained, and LPS-immunotolerant monocytes and RNA sequencing and ChIP sequencing data of control and β-glucan-trained monocytes reported in this paper have been deposited in the NCBI Gene Expression Omnibus under accession numbers GEO: GSE85246, GSE85245, GSE85243.